3. T. Kaufman, M. Seeger, G. Olsen, *Adv. Genet.* **27**, 309 (1990).
4. E. Lewis, *Nature* **276**, 565 (1978).
5. R. White and M. Akam, *ibid.* **318**, 567 (1985).
6. F. Karch, W. Bender, B. Weiffenbach, *Genes Dev.* **4**, 1573 (1990).
7. S. Celniker, D. Keelan, E. Lewis,, *ibid.* **3**, 1424 (1989).
8. R. Mann and D. Hogness, *Cell* **60**, 597 (1990).
9. S. Qian, M. Capovilla, V. Pirotta, *EMBO J.* **10**, 1415 (1991).
10. ———, *ibid.*, **12**, 3865 (1993).
11. C. Zhang, J. Müller, M. Hoch, H. Jäckle, M. Bienz, *Development* **113**, 1171 (1991).
12. R. White and R. Lehmann, *Cell* **47**, 311 (1986).
13. K. Harding and M. Levine, *EMBO J.* **7**, 205 (1988).
14. V. Irish, A. Martinez-Arias, M. Akam, *ibid.* **8**, 1527 (1989).
15. D. Lindsley and G. Zimm, Eds., *The Genome of* Drosophila melanogaster (Academic Press, San Diego, CA, 1992).
16. J. Reinitz and M. Levine, *Dev. Biol.* **140**, 57 (1990).
17. I. Duncan, personal communication; J. Simon, unpublished results.
18. The paradoxical transformation of haltere to wing may be caused by a low level of ABD-A protein that represses *Ubx* but is not high enough to transform cells to A2. As a result, a *Ubx* loss-of-function transformation is observed.
19. L. Frischer, F. Hagen, R. Garber, *Cell* **47**, 1017 (1986).
20. E. Jorgenson and R. Garber, *Genes Dev.* **1**, 544 (1987).
21. S. Celniker and E. Lewis, *Proc. Natl. Acad. Sci. U.S.A.* **90**, 1566 (1993).
22. H. Gyurkovics, J. Gausz, J. Kummer, F. Karch, *EMBO J.* **9**, 2579 (1990).
23. D. Cribbs, A. Pattatucci, M. Pultz, T. Kaufman, *Genetics* **132**, 699 (1992).
24. F. Karch, W. Weiffenback, J. Simon, W. Bender, unpublished data.
25. J. Simon, M. Peifer, W. Bender, M. O'Connor, *EMBO J.* **9**, 3945 (1990).
26. J. Simon, A. Chiang, W. Bender, M. J. Shimell, M. O'Connor, *Dev. Biol.* **158**, 134 (1993).
27. An EMBL3 library was constructed from *Hab-1* homozygotes, and the *Hab-1* containing phage was identified by hybridization with the 11.0-kb Sal I fragment illustrated in Fig. 2A. The *Hab-1* and Canton S 1.7-kb Sal I–Xba I subfragments from the 11.0-kb Sal fragment were cloned into the *Ubx/LacZ* reporter vector described by Qian, Capovilla, and Pirrota (*9*) and integrated into the *Drosophila* genome by P element–mediated germline transformation [G. M. Rubin and A. C. Spradling, *Science* **218**, 348 (1982)]. The w^+ transformant lines were established and examined for *LacZ* expression by in situ hybridization [D. Tautz and C. Pfeifle, *Chromosoma* **98**, 81 (1989)] or by staining with anti–β-galactosidase antibody (*25*). Antisense *LacZ* RNA was prepared from a pBluescript II KS(+) vector (Stratagene) containing the *LacZ*-coding region. The plasmid was linearized with Eco RI, and the digoxygenin-labeled *LacZ* probe was prepared by T7 transcription in the presence of digoxigenin uridine triphosphate. Hybridizations, washes, and histochemical staining were performed according to the procedures of J. Jiang, D. Kosman, T. Ip, and M. Levine [*Genes Dev.* **5**, 1881 (1991)]. Embryos were mounted in a solution of 70% glycerol for photography.
28. The 1.7-kb Sal I–Xba I fragment shown in Fig. 2A was subcloned in Bluescript II KS+ (Stratagene) and sequenced with standard methods. The background chromosome from bx^6/*Df(P2)* flies was also cloned and sequenced. The bx^6 allele was obtained in the same mutagenic screen as *Hab-1* and should be isogenic to *Hab-1* at all bases except for that which represents the *Hab-1* lesion (E. B. Lewis, personal communication). Chromosomal DNA from *Hab-2/Df(P2)* flies was amplified by PCR with the use of the 1-2 and 3-4 pairs of primers indicated in Fig. 2B. To eliminate PCR artifacts, the amplified products were sequenced directly with the use of the Silver sequence system (Promega, Madison, WI). The background chromosome for *Hab-2* was Canton S, and its entire 1.7-Kb Sal I–Xho I fragment was sequenced by standard methods.
29. To examine the effects of gap and pair-rule gene products on the expression of the *iab-2(1.7)* fragment, transformant lines containing this construct where crossed into the following mutant backgrounds: hb^{14F}, Kr^2, kni^{IID}, gt^{YA}, tll^{110} eve^{R13}, and *Df(2R) Scb (ftz)*. All mutants except *ftz* altered the pattern, but only *Kr* mutants showed an expression pattern reminiscent of that produced by the *Hab* mutants.
30. J. Treisman and C. Desplan, *Nature* **341**, 335 (1989).
31. M. Shimell and M. O'Connor, unpublished data.
32. M. Pankratz and H. Jäckle, in *The Development of* Drosophila melanogaster, M. Bate and A. Martinez-Arias, Eds. (Cold Spring Harbor Laboratory Press, Cold Spring Harbor, NY, 1993), pp. 467–517.
33. U. Rosenberg *et al.*, *Nature* **319**, 336 (1986).
34. F. Sauer and H. Jäckle, *ibid.* **364**, 454 (1993).
35. H. Kazazian *et al.*, *Cold Spring Harbor Symp. Quant. Biol.* **51**, 371 (1986).
36. M. Berry, F. Grosveld, N. Dillon, *Nature* **358**, 499 (1992).
37. D. Curtis, S. Clark, A. Chovnick, W. Bender, *Genetics* **122**, 653 (1989).
38. W. Driever, G. Thomas, C. Nüsslein-Volhard, *Nature* **340**, 363 (1992).
39. KR protein was produced in BL21 (DE3) cells containing plasmid pARKr [D. Stanojevic, T. Hoey, M. Levine, *ibid.* **341**, 331 (1989)]. Protein extracts were prepared from cells containing or lacking the pARKr plasmid [F. Studier, A. Rosenberg, J. Dunn, J. Dubendorff, *Methods Enzymol.* **185**, 60 (1990), as modified by T. Hoey and M. Levine, *Nature* **332**, 858 (1988)]. Protein determinations were made with the Pierce BCA protein assay kit. For footprinting experiments, DNA fragments were end-labeled with ^{32}P by a Klenow fill-in reaction. The footprinting procedure was carried out as described by Stanojevic *et al.* (above). with the following changes: The 50-ml binding reaction was composed of 100 mM KCl, 35 mM Hepes (pH 7.9), 10 mM $MgCl_2$, 1 mM dithiothreitol, 0.1 mM $ZnCl_2$, 12% glycerol, and 0.06% Nonidet P-40 and included 50,000 counts of end-labeled DNA, 2 μg of poly (dI-dC) (Pharmacia), and 5 μl of protein extract in 4 M urea and Z buffer (T. Hoey and M. Levine, above). Either 24 or 48 ng of DNase I was used in the footprinting reactions, which proceeded for 4 min on ice and were stopped by the addition of EDTA (to 50 mM) and phenol. The reactions were electrophoresed in 6% polyacrylamide–8 M urea wedge gels. The sequencing reactions were a modified version of A. Maxam and W. Gilbert [D. Bencini, G. O'Donovan, J. Wild, *BioTechniques* **2**, 4 (1984)].

40. We thank E. Lewis and I. Duncan for sharing mutant stocks and for many informative discussions on the origin and properties of *Hab* mutations; special thanks is also due to I. Duncan for suggesting that we look at the penetrance of the *Hab* phenotype in a *Kr* heterozygote. We also thank J. Treisman and C. Desplan for the antisense *LacZ* plasmid; C. Desplan for the pARKr plasmid; T. D. Nguyen for making a nested deletion series for the sequencing of the Canton S *iab-2(1.7)* fragment; and L. Marsh and R. Warrior for comments on the manuscript. Supported by grants from PHS (M.B.O. and W.B.), a fellowship from the Medical Foundation/Charles King Trust (J.S.), and a University of Minnesota McKnight Land grant (J.S.).

13 December 1993; accepted 29 March 1994

Cloning of a Grb2 Isoform with Apoptotic Properties

Isabelle Fath, Fabien Schweighoffer, Isabelle Rey, Marie-Christine Multon, Janine Boiziau, Marc Duchesne, Bruno Tocqué*

Growth factor receptor–bound protein 2 (Grb2) links tyrosine-phosphorylated proteins to a guanine nucleotide releasing factor of the son of sevenless (Sos) class by attaching to the former by its Src homology 2 (SH2) moiety and to the latter by its SH3 domains. An isoform of *grb2* complementary DNA (cDNA) was cloned that has a deletion in the SH2 domain. The protein encoded by this cDNA, Grb3-3, did not bind to phosphorylated epidermal growth factor receptor (EGFR) but retained functional SH3 domains and inhibited EGF-induced transactivation of a Ras-responsive element. The messenger RNA encoding Grb3-3 was expressed in high amounts in the thymus of rats at an age when massive negative selection of thymocytes occurs. Microinjection of Grb3-3 into Swiss 3T3 fibroblasts induced apoptosis. These findings indicate that Grb3-3, by acting as a dominant negative protein over Grb2 and by suppressing proliferative signals, may trigger active programmed cell death.

We screened 500,000 recombinant phages carrying DNA from human placenta with an oligonucleotide probe derived from the human *grb2* sequence (*1*). Nine of ten clones contained inserts that were identical to the *grb2* sequence; however, we identified one clone with a deletion in the SH2 domain (*2*). Analysis of the remaining sequence revealed an identity with *grb2*, even in the 5′ and 3′ noncoding regions. The open reading frame of the cloned DNA encoded a 177–amino acid sequence with two SH3 domains flanking the incomplete SH2 domain (Fig. 1). The amino acids deleted in the SH2 domain (amino acids 60

Rhône-Poulenc Rorer, Centre de Recherche de Vitry-Alfortville, 13 quai Jules Guesde-BP14, 94403 Vitry sur Seine Cedex, France.

*To whom correspondence should be addressed.

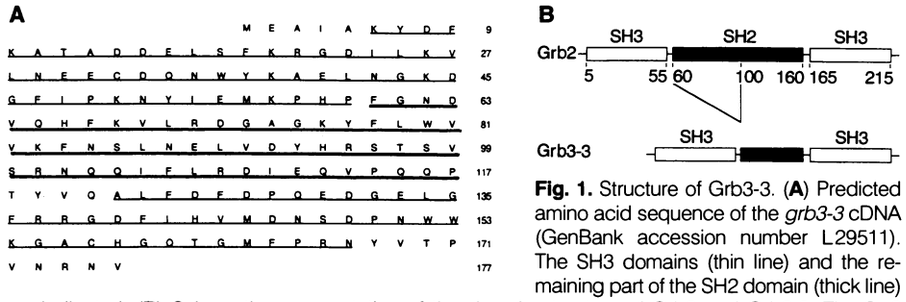

Fig. 1. Structure of Grb3-3. (**A**) Predicted amino acid sequence of the *grb3-3* cDNA (GenBank accession number L29511). The SH3 domains (thin line) and the remaining part of the SH2 domain (thick line) are indicated. (**B**) Schematic representation of the domain structure of Grb2 and Grb3-3. The SH3 regions are shown as open boxes and the SH2 regions as solid boxes. Abbreviations for the amino acid residues are as follows: A, Ala; C, Cys; D, Asp; E, Glu; F, Phe; G, Gly; H, His; I, Ile; K, Lys; L, Leu; M, Met; N, Asn; P, Pro; Q, Gln; R, Arg; S, Ser; T, Thr; V, Val; W, Trp; and Y, Tyr.

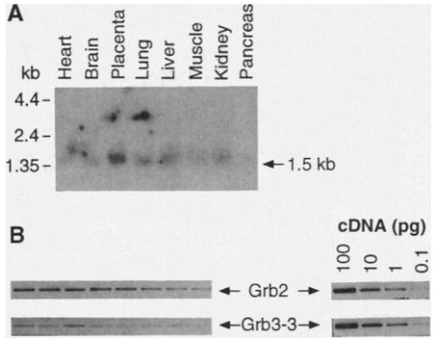

Fig. 2. Tissue expression of Grb3-3. (**A**) Northern analysis of human tissues with poly(A)$^+$ RNA of indicated origin (Commercial Multiple Northern Blot Clontech, MTN7760-1). The *grb3-3*–specific oligonucleotide ATC GTT TCC AAA CGG ATG TGG TTT, complementary to nucleotides 201 to 225, was radiolabeled (*2, 26*). Size markers are shown and the 1.5-kb Grb3-3 mRNA is indicated with an arrow. (**B**) PCR analysis of the relative expression of Grb2 and Grb3-3 mRNAs in human tissues. Poly(A)$^+$ RNA (1 μg) from the various tissues (Clontech) was reverse transcribed with a cDNA synthesis kit (Boehringer Mannheim). We then subjected 10% of the cDNA product to PCR with two different pairs of primers described below. The figure depicts 10% of the PCR products separated on a 1.5% agarose gel. To estimate the proportion of Grb3-3 mRNA, we subjected cDNA to PCR with the 5′ oligonucleotide 192 to 216, ATA GAA ATG AAA CCA CAT CCG TTT, and the 3′ oligonucleotide II (*2*). A 370–base pair (bp) fragment was amplified in all samples. These primers were shown to be specific for Grb3-3 mRNA because no band was amplified when *grb2* cDNA at concentrations ranging from 100 to 0.1 pg was used as template. To estimate the proportion of Grb2 mRNA, we performed the PCR experiments with the 3′ oligonucleotide II (*2*) and the 5′ oligonucleotide TGG TTT TTT GGCAAAATCCCCAGA. This 5′ oligonucleotide is specific for Grb2 mRNA as it hybridizes with the portion of the SH2 domain deleted in Grb3-3 (*1*). A 470-bp fragment was amplified in all samples. A titration curve (right panel) was also drawn to quantitate the ratios of Grb3-3 mRNA to Grb2 mRNA. The *grb2* or *grb3-3* cDNAs at concentrations ranging from 100 to 0.1 pg were amplified by PCR, with the pairs of primers described above. The resulting products reflected the relative proportions of Grb2 and Grb3-3 in mRNA samples.

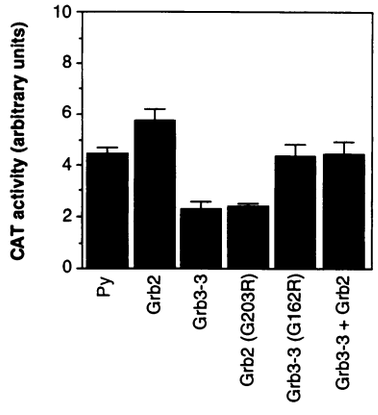

Fig. 3. Effect of Grb3-3 and Grb2 on EGF-dependent transactivation of an RRE from the polyoma virus enhancer. The cDNA sequences corresponding to the different proteins indicated were inserted into a pSV2 expression vector, downstream of the SV40 early promoter and enhancer (*29*). These plasmids were transfected into ER22 cells (*16*) with another vector containing the *cat* gene under the control of a Py-TK promoter (Py-TK-CAT). This synthetic promoter contains four head-to-tail copies of the PEA1 binding site of the polyoma enhancer upstream of the TK promoter. Transactivation of the RRE was measured after EGF stimulation. Columns represent CAT activity in cells transfected with Py-TK-CAT alone (Py), sequences encoding Grb2 (2 μg), Grb3-3 (2 μg), Grb2 (G203R) (2 μg), or Grb3-3 (G162R) (2 μg), or both Grb3-3 (2 μg) and Grb2 (2 μg). Cells at 40% confluence were transfected for 4 hours in serum-free medium with Py-TK-CAT (0.5 μg) and 2 μg of the appropriate expression vector. Total DNA was adjusted to 5 μg with expression vector without insert. Lipospermine (Transfectam, IBF-Sepracor) was used as the transfecting agent. After 24 hours of transfection, cells were stimulated with EGF (100 ng/ml). The CAT activity was determined as described (*30*) 48 hours after transfection and culture in Dulbecco's modified Eagle's medium supplemented with fetal calf serum (0.5%). Data were recorded in arbitrary units; the basal signal due to activity of the reporter gene alone in cells not stimulated with EGF was assigned a value of 1.

to 100 in Grb2) were the conserved residues that participate in the binding of phosphotyrosine-containing peptides (*3*).

By Northern (RNA) blot analysis of human tissues, mRNAs of 3.5 and 1.5 kb were detected with a full-length *grb2* cDNA probe (*1, 4*). An oligonucleotide probe specific for *grb3-3* (complementary to nucleotides 201 to 225) hybridized with a single 1.5-kb mRNA species (Fig. 2A).

Because a specific *grb2* probe (corresponding to the SH2 sequence deleted in Grb3-3) detected mRNA of both sizes (*4*), it is likely that an mRNA of about 1.5 kb encodes Grb2 and that another mRNA of the same size encodes Grb3-3. We used quantitative polymerase chain reaction (PCR) experiments to evaluate the relative abundance of Grb2 and Grb3-3 mRNA in various tissues (Fig. 2B). As suggested from the results of Northern blot analysis, Grb3-3 is widely expressed, and under the PCR conditions used, the ratio of Grb2 to Grb3-3 mRNAs ranged from 10 to 50 (Fig. 2B). It is noteworthy that the deleted SH2 sequence corresponds to one exon in both the *Caenorhabditis elegans sem5* and *Drosophila drk* genes (*5, 6*). The Grb3-3 mRNA is likely to be a splicing product of the *grb2* gene, because the remaining coding sequence and the noncoding sequences of both cDNAs are identical (Fig. 1) (*1*).

The SH2 domain of Grb2 binds to the phosphorylated receptor, and the SH3 domains interact with hSos (*6–11*). In contrast to Grb2, Grb3-3 failed to bind tyrosine-phosphorylated EGFR (*12*). Both Grb2 and Grb3-3 bound to a proline-rich peptide derived from hSos1 (*12*). These proteins failed to interact with another proline-rich peptide derived from 3BP1, which binds to the SH3 region of Abl and Src (*13, 14*). A mutation (G203R) that affects a highly conserved residue in the SH3 domain of Grb2 impairs the binding of this protein to hSos1 (*9*) and its ability to activate Ras in a DNA synthesis reinitiation assay (*1*). In our binding assay, Grb3-3 (G162R), containing the equivalent mutation, failed to interact with the hSos1 peptide, indicating that the interaction between Grb3-3 and hSos1 required the SH3 domains (*12*).

To study if Grb2 and Grb3-3 both connect the EGFR to the Ras pathway, we overexpressed these proteins and measured EGF-dependent transactivation of Ras-responsive element (RRE) contained in the polyoma enhancer (Py) (*15*). Chinese hamster lung fibroblasts overexpressing the human EGFR (ER22 cells) (*16*) were cotransfected with a plasmid containing the chloramphenicol acetyltransferase (CAT) gene under the control of the Py–thymidine kinase promoter (Py-TK-CAT) and with expression vectors containing *grb2* or *grb3-3* cDNAs under the control of the SV40 early

promoter (Fig. 3). Grb2 enhanced the response to EGF by 40%. In contrast, Grb3-3 reduced by 50% the CAT expression stimulated by EGF. Cotransfection of an excess of Grb2 overcame the inhibitory effect of Grb3-3 (Fig. 3). In the absence of EGF, neither Grb2 nor Grb3-3 induced CAT expression (*17*).

To further characterize the involvement of the SH3 domains in the dominant negative effect of Grb3-3, we transfected cells with the mutant encoding Grb3-3 (G162R). This mutant had no effect on EGFR-mediated signal transduction (Fig. 3). In contrast, the mutant Grb2 (G203R) did inhibit stimulation of CAT expression by EGF, probably by competing with cellular Grb2 for binding to phosphorylated EGFR. The coexistence of two complexes in the cytosol, Grb2-Sos and Grb3-3–Sos, can be proposed. Upon EGF stimulation, only the Grb2-Sos complex would be able to mediate EGF signaling by means of a specific SH2-dependent interaction; the Grb3-3–Sos complex would remain insensitive to EGF. Depending on the ratios of Grb2 to Grb3-3 and on the relative affinities of these proteins for Sos or other targets, Grb3-3 might serve as a suppressor of Grb2 function.

The mutations *Su(Sev^{s11})R1* and *E(sev)2B* in the SH2 domain of the *Drosophila grb2* homolog, *drk*, cause recessive lethality (6). Such mutations can be rescued by ubiquitous expression of *drk* cDNA, suggesting a critical balance between the wild-type and the mutant adaptors. The relative abundance of Grb3-3 and Grb2 might affect cell signaling and viability. However, in adult tissues, Grb3-3 mRNA is much less abundant than Grb2 mRNA (Fig. 2). We therefore compared expression of mRNAs encoding Grb3-3 and Grb2 during ontogeny of the rat thymus. Expression of Grb3-3 mRNA varied with the age of the thymus, whereas expression of Grb2 mRNA remained constant (Fig. 4). Quantitative PCR analysis showed that the amount of Grb3-3 mRNA reached a peak at 5 weeks. At this stage of development, the ratio of Grb3-3 mRNA to Grb2 mRNA was 1 to 1 (Fig. 4). Grb3-3 seems therefore to be present in sufficiently large amounts to compete with Grb2 at a time when maturation and cell death occur (*18*). Expression of Grb2 and Grb3-3 did not vary during the same period in brain or heart where Grb3-3 was barely expressed (*19*). The Bclx-s mRNA, which encodes a protein involved in thymocyte and lymphocyte apoptosis (*20*), is most abundant in rat thymus at the same time during development (Fig. 4). Our results reveal similarities between the *grb2* and the *bclx* gene families. Expression of the *bclx* gene, a *bcl2*-related gene, results in two distinct mRNAs, Bclx-l and Bclx-s. The two products result from alternative splicing and have opposite effects on cell survival (*20*).

We tested whether Grb3-3 was able to trigger apoptosis when present in excess over Grb2. Recombinant Grb3-3 was microinjected into confluent Swiss 3T3 fibroblasts. Grb3-3 was toxic to the cells, inducing extensive cell death within 5 to 12 hours (Fig. 5). Microinjection of Grb2 or Grb3-3 (G162R) at the same concentration had no effect (*21*). Time-lapse video recording showed that cells injected with Grb3-3 underwent a death process highly reminiscent of apoptosis, with progressive condensation of the cytoplasm around the nucleus and intense cell shrinkage (Fig. 5, A through C). The cells eventually rounded up and detached from the dish. Propidium iodide staining of the DNA showed that a number of cells injected with Grb3-3 displayed a small, brightly stained and highly condensed nucleus. Chromatin was aggregated into dense masses at the periphery of the nucleus (Fig. 5D) and, in some cases, fragmented as evidenced by patches of condensed chromatin underlying the nuclear membrane (Fig. 5E). Under phase contrast, these cells appeared shrunken (*21*). Consistent with the CAT assays, Grb2, but not Grb2 (G203R), microinjected in a 10-fold excess over Grb3-3 overcomes the effect of Grb3-3 in apoptotic response (*21*).

Grb3-3 could act as a mediator of apoptosis by forming an inactive heterodimeric complex with the Sos protein or other alternative partners and thus act as a dominant inhibitor of Grb2 function. However, Grb3-3 could also act by triggering a specific apoptotic signal within the cells. The fact that a dominant negative Ha-Ras Asn^{17} mutant (*22*), which has been shown to act by sequestering Ras exchange factor (*23*), does not induce apoptosis (*24*) suggests that titration of Sos is not sufficient for inducing apoptosis and that Grb3-3 has other targets besides Sos.

Our findings indicate that Grb3-3 may function in the regulation of programmed cell death in the thymus and possibly in other tissues. Other SH2-containing adaptors, such as Nck and Shc (*25*), have been described. If altered forms of these proteins also exist,

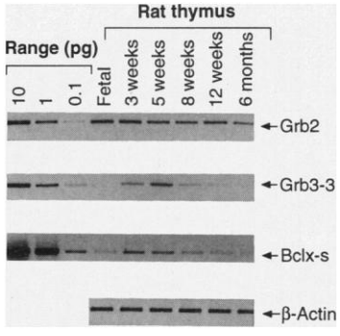

Fig. 4. Analysis of relative proportions of Grb2 and Grb3-3 mRNAs expressed during development of the rat thymus. Total RNA was prepared with RNA zol (Bioprobe system) from whole thymuses of rats at various ages, as indicated. Total RNA (20 μg) was reverse transcribed and 10% of the cDNA product was then subjected to PCR as described (Fig. 2B). Also shown are the relative amounts of *grb2* and *grb3-3* that were produced with known amounts of rat *grb2* and *grb3-3* cDNAs as templates (*31*). In addition, 10% of the cDNA product was used for PCR with *bclx-s*–specific primers derived from the published sequence (*20*). Cloned *bclx-s* cDNA was used as template for the titration experiments. As a control to ensure that the same amount of cDNA was used in all experiments, the cDNA encoding β-actin was amplified by PCR with specific oligonucleotides (*32*).

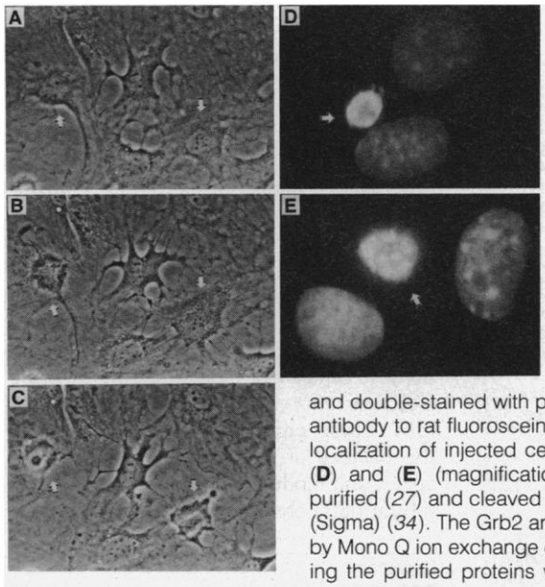

Fig. 5. Induction of apoptosis in quiescent Swiss 3T3 cells by Grb3-3. Purified Grb3-3 was injected into cells (1 to 3 mg/ml) with an automatic Eppendorf microinjector. Cells were then incubated at 34°C, and photographs were taken at regular intervals. Pictures taken 4.5, 5, and 5.3 hours after injection are shown in (**A**), (**B**), and (**C**), respectively (magnification, ×78). To assess the effect of Grb3-3 on DNA, we grew cells on glass coverslips and coinjected them with Grb3-3 along with rat immunoglobulin (2 mg/ml) as a marker. They were fixed 6 to 7 hours after injection and double-stained with propidium iodide as described (*33*) and antibody to rat fluoroscein isothiocynate (Pierce) to allow specific localization of injected cells. Representative fields are shown in (**D**) and (**E**) (magnification, ×390). GST fusion proteins were purified (*27*) and cleaved by addition of human thrombin (0.25%) (Sigma) (*34*). The Grb2 and Grb3-3 proteins were further purified by Mono Q ion exchange chromatography. The fractions containing the purified proteins were concentrated in Microsep microcentrators (Filtron) in 20 mM phosphate buffer (pH 7) containing 100 mM NaCl.

deletion within the SH2 domain might represent a general mechanism by which cells regulate signaling and the cascade of connections that occur by means of phosphotyrosine-containing proteins and adaptors.

REFERENCES AND NOTES

1. E. J. Lowenstein *et al.*, *Cell* **70**, 431 (1992).
2. The oligonucleotide ATGGAAGCCATCGCCAA-ATATGAC, corresponding to the first eight amino acids of the Grb2 protein (*1*), was used to screen (*26*) 500,000 phages from a human placenta λgt11 library (Clontech). The lambda DNA fragments from the 10 positive clones were digested with Eco RI and cloned in M13mp18 vectors. After sequencing, the open reading frames of *grb2* and *grb3-3* were amplified by PCR with the 5′ oligonucleotide I:GCCGGATCCATGGAAGCCATCGC-CAAATATGACTTC and the 3′ oligonucleotide II:GCCGGATCCTTAGACGTTCCGGTTCACGG-GGGTGAC, where Bam HI sites followed by the natural start or stop codons are underlined. The PCR-amplified Bam HI fragments of *grb2* and *grb3-3* were cloned into pGEX-2T (Pharmacia) digested with Bam HI to produce glutathione-S-transferase (GST) fusion proteins in *Escherichia coli* (*12*). The same fragments were also cloned into Bgl II–digested pSV2 for transient transfection studies (Fig. 3). The mutants *grb2* (G203R) and *grb3-3* (G162R) were obtained by PCR-mediated mutagenesis with the 5′ oligonucleotide I described above and the 3′ oligonucleotide GAC GTT CCG GTT CAC GGG GGT GAC ATA ATT GCG GGG AAA CAT GCG GGT C, where the mutated codon is underlined. The PCR-amplified fragments were eluted and reamplified by PCR with oligonucleotides I and II. They were then cloned in pGEX-2T and pSV2 expression vectors, as were wild-type *grb2* and *grb3-3*. All fragments amplified by PCR were sequenced.
3. G. Waksman *et al.*, *Nature* **358**, 646 (1992).
4. I. Fath *et al.*, unpublished data. The commercial Northern blot, described in Fig. 2A, was dehybridized and rehybridized either with a full-length *grb2* cDNA or with a fragment specific for *grb2*. These fragments were radiolabeled with a random-primed labeling kit (Boerhinger Mannheim). We detected mRNAs of 3.5 and 1.5 kb.
5. S. G. Clark, M. J. Stern, H. R. Horvitz, *Nature* **356**, 340 (1992).
6. J. P. Olivier *et al.*, *Cell* **73**, 179 (1993).
7. S. E. Egan *et al.*, *Nature* **363**, 45 (1993).
8. M. Rozakis-Adcock, R. Fernley, J. Wade, T. Pawson, D. Bowtell, *ibid.*, p. 83.
9. N. Li *et al.*, *ibid.*, p. 85.
10. N. W. Gale, S. Kaplan, E. J. Lowenstein, J. Schlessinger, D. Bar-Sagi, *ibid.*, p. 88.
11. L. Buday and J. Downward, *Cell* **73**, 611 (1993).
12. Grb3-3 did not bind to phosphorylated EGFR. Nonphosphorylated EGFR and phosphorylated EGFR were blotted and probed with biotinylated GST-Grb2, GST–Grb3-3, GST–Grb3-3(G162R), or GST, showing that the binding of Grb2 to phosphorylated EGFR in vitro required SH2 domains. GST fusion proteins were purified and biotinylated according to published procedures (*27*). EGFR purified from A431 cells (*28*) on wheat germ agglutinin–Sepharose (2 μg) was first stimulated with 1 μM EGF for 10 min at 22°C and further incubated with or without cold adenosine triphosphate (ATP) (10 μM) in the presence of 2.5 mM $MnCl_2$ in HNTG buffer [20 mM Hepes (pH 7.5), 150 mM NaCl, 0.1% Triton, and 10% glycerol] at 4°C for 2 min. Samples were run on an SDS-polyacrylamide gel (4 to 20%) and transferred to polyvinylidene difluoride (PVDF) membrane. Blots were probed with biotinylated GST-Grb2, GST–Grb3-3, GST–Grb3-3(G162R), or GST (2 μg/ml), and bound proteins were detected with streptavidin coupled to alkaline phosphatase (Promega). We also subjected EGFR proteins to immunoblotting with antibodies to phosphotyrosine; Grb2 and Grb3-3 bound to a proline-rich peptide from hSos1 but not to a proline-rich peptide from 3BP1. Two proline-rich peptides were synthesized: 3BP1 peptide PPPLPPLV (*13, 14*) and hSos1 peptide GTPEVPVPPPVPPRRRPESA (*9*). Each peptide (1 μl, 10 mg/ml) was spotted onto nitrocellulose membranes. Membranes were incubated in blocking buffer [20 mM tris (pH 7.6), 150 mM NaCl, 0.1% Tween 20, and 3% bovine serum albumin]. The membranes were probed with biotinylated GST-Grb2, GST–Grb3-3, GST–Grb3-3(G162R), or GST (4 μg/ml) overnight at 4°C. Positive reactions were identified with streptavidin coupled to alkaline phosphatase.
13. P. Cicchetti, B. J. Mayer, G. Thiel, D. Baltimore, *Science* **257**, 803 (1992).
14. R. Ren, B. J. Mayer, P. Cicchetti, D. Baltimore, *ibid.* **259**, 1157 (1993).
15. F. Schweighoffer, I. Barlat, M. C. Chevallier-Multon, B. Tocqué, *ibid.* **256**, 825 (1992).
16. G. L'allemain, K. Seuwen, T. Velu, J. Pouyssegur, *Growth Factors* **1**, 311 (1989).
17. I. Fath *et al.*, unpublished data. When cells were transfected with *grb2* or *grb3-3* plasmid and not stimulated with EGF, the basal signal due to the reporter gene alone was not modified.
18. R. G. Scollay, E. C. Butcher, I. L. Weissman, *Eur. J. Immunol.* **10**, 210 (1980).
19. I. Fath *et al.*, unpublished data. The quantitative PCR experiments, described in Fig. 5, were also carried out with cDNA prepared from brain and heart of the same rats. In these tissues, *grb2* and *grb3-3* were expressed at every age in the same proportion as in adult.
20. L. H. Boise *et al.*, *Cell* **74**, 597 (1993).
21. I. Rey, unpublished data.
22. L. A. Feig and G. M. Cooper, *Mol. Cell. Biol.* **8**, 3235 (1988).
23. F. Schweighoffer *et al.*, *ibid.* **13**, 39 (1993).
24. R. G. Sosnowski, S. Feldman, J. R. Feramisco, *J. Cell. Biol.* **121**, 113 (1993).
25. G. Pellici *et al.*, *Cell* **70**, 93 (1992); J. M. Lehman, G. Riethmuller, J. P. Johnson, *Nucleic Acids Res.* **18**, 1048 (1990).
26. J. Sambrook, E. F. Fritsch, T. Maniatis, *Molecular Cloning: A Laboratory Manual* (Cold Spring Harbor Laboratory Press, Cold Spring Harbor, NY, 1989).
27. B. J. Mayer, P. K. Jackson, D. Baltimore, *Proc. Natl. Acad. Sci. U.S.A.* **88**, 627 (1991); M. Duchesne *et al.*, *Science* **259**, 525 (1993).
28. A. Gazit, P. Yaish, C. Gilon, A. Levitzki, *J. Med. Chem.* **32**, 2344 (1989).
29. C. Wasylyk, J. L. Imler, J. L. Chatton, C. Schatz, B. Wasylyk, *EMBO J.* **7**, 7952 (1988).
30. C. M. Gorman, L. F. Moffat, B. H. Howard, *Mol. Cell. Biol.* **2**, 1044 (1982).
31. K. Matuoka, M. Shibata, A. Yamakawa, T. Takenawa, *Proc. Natl. Acad. Sci. U.S.A.* **89**, 9015 (1992).
32. R. A. Montgomery and M. J. Dallman, *J. Immunol.* **147**, 554 (1991).
33. M. D. Jacobson *et al.*, *Nature* **361**, 365 (1993).
34. K. L. Guan and J. E. Dixon, *Anal. Biochem.* **192**, 262 (1991).

35. We thank F. Risbec and K. Pepper for assistance and P. F. Berne for purification of Grb3-3. Supported by the BioAvenir Program (Ministère de la Recherche et de l'Espace, Ministère de l'Industrie et du Commerce Extérieur).

17 December 1993; accepted 29 March 1993

Activity-Dependent Changes in the Intrinsic Properties of Cultured Neurons

Gina Turrigiano,* L. F. Abbott, Eve Marder

Learning and memory arise through activity-dependent modifications of neural circuits. Although the activity dependence of synaptic efficacy has been studied extensively, less is known about how activity shapes the intrinsic electrical properties of neurons. Lobster stomatogastric ganglion neurons fire in bursts when receiving synaptic and modulatory input but fire tonically when pharmacologically isolated. Long-term isolation in culture changed their intrinsic activity from tonic firing to burst firing. Rhythmic stimulation reversed this transition through a mechanism that was mediated by a rise in intracellular calcium concentration. These data suggest that neurons regulate their conductances to maintain stable activity patterns and that the intrinsic properties of a neuron depend on its recent history of activation.

The outputs of neural circuits depend both on synaptic connections and on the intrinsic electrical properties of individual neurons (*1*). Activity-dependent modification of synaptic strengths contributes to processes such as developmental segregation of inputs and learning (*2*) and has been well described. Less extensively studied has been the role of activity in shaping the intrinsic electrical properties of neurons [but see (*3*)]. These properties are determined by the balance of a neuron's ionic conductances, and modification of this balance can substantially change the output of the circuits in which a neuron participates (*1, 4*). Here we show that activity can alter the intrinsic electrical properties of neurons, which suggests that a neuron's physiological identity is influenced by the synaptic input it receives.

We studied stomatogastric ganglion (STG) neurons from the spiny lobster, *Panulirus interruptus*, that participate in two motor programs producing rhythmic movements of the teeth and foregut. This rhythmic activity depends both on modulatory and rhythmic inhibitory synaptic drives that cause STG neurons to fire bursts of action potentials when released from inhibition. When pharmacologically isolated, STG neurons do not fire in bursts but fire tonically (Fig. 1A) (*4*).

Department of Biology and Center for Complex Systems, Brandeis University, Waltham, MA 02254, USA.

*To whom correspondence should be addressed.